Journal of Cardiovascular Magnetic Resonance (2005) **7,** 809–814

ISSN: 1097-6647 print / 1532-429X online
DOI: 10.1080/10976640500287786

Taylor & Francis
Taylor & Francis Group

ANGIOGRAPHY

MR coronary angiography using 3D-SSFP with and without contrast application

ANJA ZAGROSEK, M.D.,[1,*] RALPH NOESKE, PH.D.,[2] HASSAN ABDEL-ATY, M.D.,[1] MATTHIAS G. FRIEDRICH, M.D., F.E.S.C.,[1,3] RAINER DIETZ, M.D.,[1] and JEANETTE SCHULZ-MENGER, M.D.[1]

[1]*Franz-Volhard-Klinik, Helios-Klinikum Berlin, Kardiologie, Charité Campus Berlin-Buch, Humboldt-Universität zu Berlin, Berlin, Germany*
[2]*GE Healthcare, Berlin, Germany*
[3]*Department of Cardiac Sciences and Radiology, University of Calgary, Calgary, Alberta, Canada*

We compared the performance of a contrast-enhanced with a non-contrast breath-hold 3D-SSFP-sequence for Magnetic Resonance Coronary Angiography in seven healthy subjects and 14 patients. Visibility of coronary segments, vessel length, image quality and the influence of an extracellular contrast agent (Gadolinium-DTPA) were assessed. Overall, the performance of the sequence was better in healthy subjects than in patients. Although the application of Gadolinium-DTPA increased the contrast-to-noise-ratio of the right coronary artery, the overall performance was not significantly improved. We conclude that a 3D-SSFP-technique depicts extensive parts of the coronary arteries and does not require contrast application.

Key Words: Magnetic resonance coronary angiography; Coronary artery imaging; Breath-hold technique; Contrast media; Three-dimensional technique; SSFP-sequence

1. Introduction

Although Magnetic Resonance Coronary Angiography (MRCA) has been under development for more than a decade (1), there is still no agreement on the type of sequence and the need for contrast application. Main challenges for MRCA include the spatial resolution, motion artifacts, tortuosity of the vessels and the proximity of pericardial fat and cardiac chambers (2–4). To overcome these problems, three-dimensional (3D) breath-hold and free-breathing MRCA techniques (5–9) have been recently introduced. Among those, steady-state free precession (SSFP) sequences appear promising because of their short repetition and echo times and excellent contrast between blood and surrounding structures (10–15). In SSFP sequences applied for MRCA, however, data are acquired while the signal is in transience to steady state and thus SNR and CNR do not reach their maximal values. Since image contrast in SSFP is primarily based upon the ratio of tissue T2/T1 relaxation times, intravascular application of a T1-shortening contrast agent increases the signal intensity of blood, and should thus lead to higher SNR and CNR values of the coronary arteries. Moreover, the rather slow washout of the contrast agent would provide a relatively long temporal window (20–30 min) of optimal contrast impact, sufficient enough for image acquisition and evading the limitations of a first-pass angiography. So far, data are only available for peripheral angiography (16).

We assessed the performance and the clinical feasibility of a breath-hold 3D-SSFP sequence to visualize the coronary arteries with and without application of an extracellular contrast agent (Gadolinium-DTPA).

2. Materials and methods

Twenty-one individuals underwent MRCA, among them seven healthy subjects and 14 patients, 1 ± 3 days after conventional X-ray coronary angiography for clinical suspicion of coronary artery disease. All participants gave written informed consent before the examination and the study was approved by the institutions local ethics committee. Special exclusion criteria were prior coronary bypass grafts or cardiac surgery with implantation of metallic clips, coronary artery stenting, severe cardiac arrhythmia and pre-existing pulmonary disease. Patients with contraindications to MR imaging

Received 7 January 2004; accepted 29 July 2005.
*Address correspondence to Anja Zagrosek, M.D., Franz-Volhard-Klinik, Working Group Cardiac MRI, Helios-Klinikum Berlin, Charité, Campus Berlin-Buch, Humboldt-Universitaet zu Berlin, Wiltbergstr. 50, Berlin D-13125, Germany; Fax: +49-30-9417-2560; E-mail: zagrosek@fvk.charite-buch.de

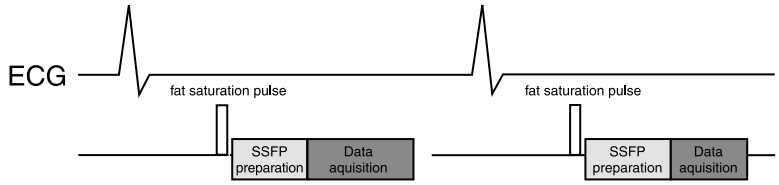

Figure 1. ECG-gated 3D-SSFP sequence (FIESTA) using the variable sampling in time approach (VAST): Each partition encoding set is acquired in two heartbeats: 32 lines are acquired in the first R-R interval and the rest in the second R-R interval (data acquisition). The spectrally selective inversion RF-pulse (fat saturation pulse) is followed by a half-alpha, half-TR preparation pulse and 6 dummy RF pulses to accelerate the approach to steady-state (SSFP preparation). The SSFP preparation phase is then followed by the data acquisition.

(automatic implantable defibrillators, pacemakers, intracranial aneurysm clip, etc) or contrast administration were excluded as well. All studies were performed on a 1.5- Tesla system (Signa CV/*i*, GE Healthcare Technologies, Milwaukee, Wisconsin, USA) with a high-performance gradient system (peak amplitude 40 mT/m, maximum slew rate 150 mT/m/ms).

2.1. *MR coronary angiography*

All subjects were examined in supine position. Data acquisition was electrocardiographically triggered and each imaging sequence was performed within one breath-hold in exspiration using a four-element, cardiac-optimized phased-array coil.

The imaging protocol for the investigational sequence consisted of two steps. First, two to three scout scans were acquired for coronary artery localization in transverse, sagittal and/or coronal orientation. For these scans an ECG-triggered multislice 2D segmented fast gradient echo sequence (TR=5.7 ms, TE=1.6 ms, matrix=256 × 160, FOV=34.0 × 25.5 mm, NEX=1, slice thickness=5 mm, no slice gap) was used, yielding 12–16 slices per breathhold. On these 2D scout images the position of the coronary arteries was determined and the double-oblique 3D-imaging planes were planned separately for the left anterior descending (LAD) coronary artery, the left circumflex (LCX) and the right coronary artery (RCA). Volume targeted breath-hold scans were then acquired in exspiration along the above-obtained orientations using the investigational 3D steady state free precession sequence (FIESTA, Fig. 1). Technical parameters were as follows: TR=4.4 ms, TE=1.8 ms, flip angle 65°, receiver bandwidth 125 kHz, NEX 0.5, matrix 256 × 192, FOV 26.0–28.0 cm, 2.2–2.6 cm slab thickness. Fat suppression was achieved by a spectrally selective inversion RF-pulse, which was played out prior to each data acquisition window. A half-alpha, half-TR preparation pulse followed by 6 dummy RF pulses was used to accelerate the approach to steady-state. The segmented data acquisition was distributed over 24 heartbeats, yielding 12 partitions. Each partition encoding set was acquired in two heartbeats using the variable sampling in time (VAST, Fig. 1) approach (17, 18). For each slice partition, the data acquisition consists of two non-equal temporal segments, which are placed at the same cardiac phase of two consecutive cardiac cycles. By acquiring the low-spatial-frequency data in a more compact acquisition window than the high-spatial-frequency k-space lines for each slice partition, cardiac motion related blurring can be reduced as compared to the standard symmetric approach. Using a matrix of 256 × 192, this leads to a VAST-ratio of 24:84, meaning that 24 k-space lines are acquired in the first and 84 k-space lines in the second RR-interval. Shimming of the magnetic field was performed prior to each scan. Trigger delays were adjusted to the subjects' heart rate so that the data acquisition was placed in middiastole between 60–80% of the RR-interval. If necessary, these scans were repeated and optimized for the vessels' exact courses. Images of the right or left coronary artery were obtained in a random order to decrease the influence of the examination's duration on image quality.

In 5 healthy subjects and in all of the patients a second scan for each coronary artery was applied with the investigational sequence after intravenous injection of Gadolinium-DTPA (Magnevist, Schering, Germany) using an automated injector (Medrad, PA). The contrast dose was 0.1–0.2 mmol/kg bodyweight of Gd-DTPA as a bolus, followed by 20 mL of normal saline. No particular imaging order of the coronary arteries was followed after application of Gd-DTPA.

Table 1. Visibility of coronary segments

Segment	Healthy subjects	Patients
LMCA	100.0% (7/7)	83.3% (10/12)
LAD1	100.0% (7/7)	83.3% (10/12)
LAD 2	100.0% (7/7)	75.0% (9/12)
LAD 3	71.4% (5/7)	25.0% (3/12)
LCX 1	83.3% (5/6)	100% (8/8)
LCX 2	0.0% (0/6)	37.5% (3/8)
LCX 3	0.0% (0/6)	0.0% (0/8)
RCA 1	100.0% (7/7)	100.0% (12/12)
RCA 2	100.0% (7/7)	91.7% (11/12)
RCA 3	100.0% (7/7)	66.6% (8/12)
Total	77.6% (52/67)	68.5% (74/108)

Segments of the coronary artery tree visualized in MRCA in patients and in healthy subjects.

Table 2. Length of the coronary arteries

Vessel	Healthy subjects	Patients	p value
LMCA	12 mm ± 3 (7–15 mm)	12 mm ± 1 (9–13 mm)	.96
LAD	75 mm ± 6 (68–82 mm)	51 mm ± 20 (29–90 mm)	.02
LCX	23 mm ± 7 (15–32 mm)	35 mm ± 12 (14–52 mm)	.10
RCA	106 mm ± 19 (79–135 mm)	84 mm ± 37 (12–134 mm)	.18

Length of the coronary arteries as visualized in MRCA, data are mean values ± SD, numbers in parentheses are ranges.

Table 3. Diameter of the coronary arteries

Vessel	Healthy subjects	Patients	p value
LMCA	3.1 mm ± 0.3 (3.1–3.5 mm)	3.8 mm ± 0.6 (3.0–4.7 mm)	.01
LAD	2.9 mm ± 0.5 (2.4–3.7 mm)	2.9 mm ± 0.4 (2.2–3.5 mm)	.89
LCX	2.5 mm ± 0.4 (1.9–3.0 mm)	2.9 mm ± 0.6 (2.2–3.2 mm)	.22
RCA	3.3 mm ± 0.5 (2.7–4.2 mm)	3.7 mm ± 0.7 (2.7–4.9 mm)	.19

Diameter of the coronary arteries as visualized in MRCA, data are mean values ± SD, numbers in parentheses are ranges.

2.2. *Image analysis*

Images were transferred to a commercially available workstation (Advantage Windows 4.0, GE Healthcare Technologies, Milwaukee, Wisconsin, USA). The image quality was determined by one observer blinded to the participants' data, based on the 2D original source data. The image quality was evaluated on a per-coronary basis and graded using a score from 1 to 4, depending on sharp vessel definition, visualization of side-branches and motion artefacts (1 = unreadable; 2 = moderate, vessel visible but not clearly demarcated from adjacent myocardium; 3 = good, vessel demarcated from adjacent myocardium; 4 = excellent, vessel borders clearly defined). The length of each coronary artery and its diameter 1 cm distal to the offspring were measured.

The coronary artery tree was subdivided into 10 segments with 3 segments of 3 cm length per coronary artery plus the left main stem, allowing for a quantification of visible segments. This approach avoids the use of side-branches to subdivide the coronary arteries (19).

2.3. *SNR and CNR measurements*

SNR and CNR were measured on images before and after the application of contrast agent in two identical slices of the source images. Blood signal (S_{Blood}) was measured in the lumen of the proximal to middle segments of the coronary arteries, with the region-of-interest (ROI) drawn within the boundaries of the vessels and then copied to the post-contrast images. The myocardial signal ($S_{Myocardium}$) was measured in close proximity to the coronaries. The standard deviation of noise was considered the mean signal intensity of air divided by a factor of 1.25 (10). SNR and CNR were then calculated as follows:

$$\mathrm{SNR} = \frac{S_{Blood} \times 1.25}{\text{Mean SI of air}} \quad (1)$$

$$\mathrm{CNR} = \frac{(S_{Blood} - S_{Myocardium}) \times 1.25}{\text{Mean SI of air}} \quad (2)$$

2.4. *Statistical analysis*

SNR and CNR values are presented as mean ± SD. A p value $< .05$ was considered statistically significant. Statistical analysis was performed using commercially available software (StatView 4.5, Abacus Concepts, Berkeley, California, USA). All statistical tests were 2 tailed. Continuous data were compared using the student t-test.

Table 4. Image quality

Vessel	Healthy subjects	Patients	p value
LMCA	3.9 ± 0.3	3.0 ± 0.6	< .05
LAD	3.0 ± 0.5	2.4 ± 0.6	< .05
LCX	1.7 ± 0.4	1.9 ± 0.5	.36
RCA	3.6 ± 0.3	3.1 ± 0.7	< .05
Overall	3.0 ± 0.3	2.4 ± 0.6	< .05

Image quality of MRCA in healthy subjects and in patients. Data are mean image quality scores ± SD (4=excellent, 3=good, 2=moderate, 1=unreadable).

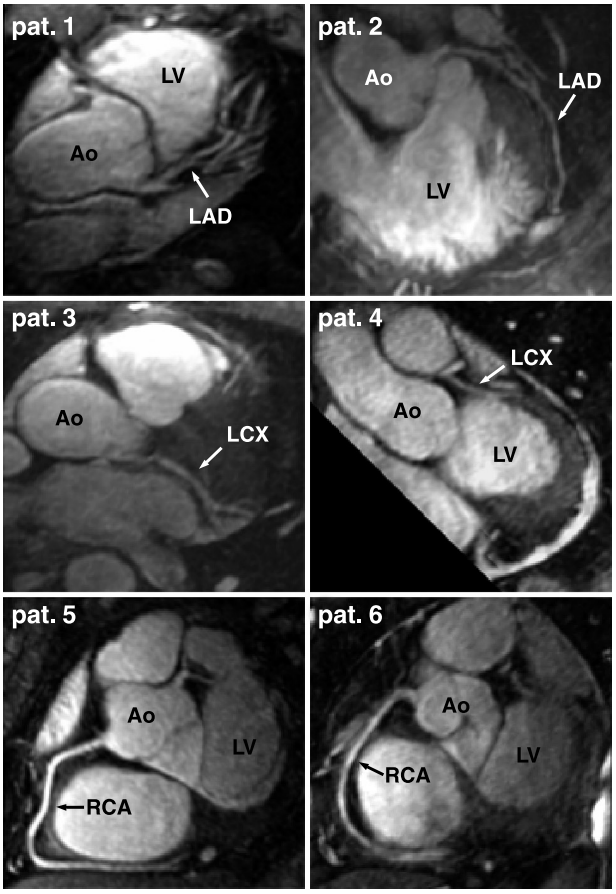

Figure 2. MIP-images of the left anterior descending coronary artery (LAD), the left circumflex coronary artery (LCX) and the right coronary artery (RCA) of 6 different patients after application of contrast agent (Gd-DTPA). Image quality of the patients, according to the score applied in this study: patients 1–4 = good (3), patients 5 and 6 = excellent (4). LV = left ventricle, Ao = Aorta.

3. Results

MRCA was completed in 7 healthy subjects (3 males) and 14 patients (8 males) without complications. All the participants were able to sustain the 24 heartbeats breath-hold. The mean age was 41 ± 14 years in healthy subjects and 67 ± 6 years in patients ($p < .05$). The mean heart rate during the breath-hold was 64.0 ± 5.3 in healthy subjects and 67.5 ± 10.2 ($p = .43$) in patients. The mean LVEF was 63.3 ± 7.4 in healthy subjects and 66.3 ± 5.1 ($p = .34$) in patients. Two patient studies revealed a non-diagnostic image quality excluding their images from further analysis.

The mean scan duration was 38 ± 14 min in healthy subjects and 44 ± 9 min in patients (p = n.s.), including localization of the heart, scout scans for coronary artery localization and accomplishment of the investigational MRCA-scans before and after application of contrast agent. The two healthy subjects not having received Gd-DTPA were excluded from the time calculations.

Seventy-two percent of the targeted vessel segments were eligible for evaluation. Imaging of the LMCA, the LAD and the RCA was accomplished in all of the participants, whereas scanning of the LCX was performed in only 6 (86%) of the healthy subjects and 8 (57%) of the patients. In summary, visualization of the targeted vessel segments was more successful in healthy subjects than in patients, although the difference did not reach statistical significance (Table 1). Generally, the more distal the vessels were, the lower the percentage of visible segments was. The RCA was the vessel to be visualized most reliably; the LCX was the most difficult vessel to assess.

The results of vessel length and diameter were strongly correlated to those of the visible coronary segments. In healthy subjects, we found an average vessel length of 12 ± 3 mm for the left main coronary artery (LMCA); 75 ± 6 mm for the LAD; 23 ± 7 mm for the LCX; and 106 ± 19 mm for the RCA. In patients, the average vessel length was 12 ± 1 mm for the LMCA; 51 ± 20 mm for the LAD; 35 ± 12 mm for the LCX; and 84 ± 37 mm for the RCA (Table 2). Except for the LAD, the differences in length between the two groups did not reach statistical significance, probably due to the substantial variability.

Data for the proximal diameters of the vessels are presented in Table 3. Although there appeared to be a distinct trend towards larger vessel calibres in patients, this difference did reach statistical significance only for the left main coronary artery.

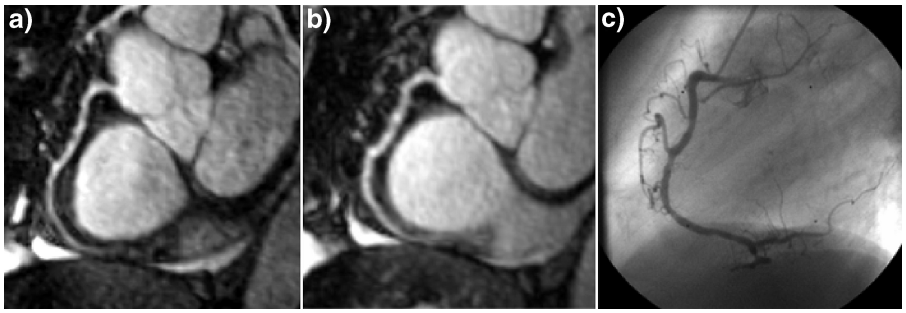

Figure 3. Comparison of MRCA and conventional X-ray angiography: a + b) MIP-images of the RCA before and after application of contrast agent (Gd-DTPA), demonstrating no significant change in image quality; c) corresponding conventional X-ray angiography.

Table 5. Influence of Gd-DTPA on SNR and CNR

		Pre-contrast	Post-contrast	p value
SNR	LAD	6.8 ± 3.1	8.8 ± 4.1	< .01
	LCX	7.6 ± 3.8	10.1 ± 2.7	< .01
	RCA	12.8 ± 5.1	17.2 ± 6.6	< .01
CNR	LAD	3.7 ± 1.5	3.8 ± 1.7	.38
	LCX	4.3 ± 2.8	4.6 ± 1.2	.36
	RCA	10.0 ± 4.5	12.7 ± 5.2	< .01

Signal-to-noise ratio (SNR) and contrast-to-noise ratio (CNR) of the left and right coronary artery (LAD, LCX and RCA) before and after application of Gd-DTPA. Data are mean signal intensity (SI).

Table 6. Overall image quality before and after application of contrast agent

Vessel	Before contrast	After contrast	p value
LMCA	3.3 ± 1.0	3.1 ± 0.9	.58
LAD	2.4 ± 1.1	2.3 ± 1.1	.64
LCX	1.8 ± 1.0	1.9 ± 1.1	.79
RCA	3.3 ± 1.0	3.4 ± 0.9	.63

Overall image quality of MRCA before and after application of contrast agent. Data are mean image quality scores ± SD (4=excellent, 3=good, 2=moderate, 1=unreadable).

Except for the LCX, the image quality was significantly better in healthy subjects than in patients (Table 4). Healthy subjects had an excellent image quality of the RCA and LMCA and a good image quality of the LAD, whereas patients presented with slightly lower values than the group of healthy subjects. Image quality of the LCX was poor with no significant differences between healthy subjects and patients. To demonstrate the image quality and the use of our 4-point-score, Fig. 2 shows MIP-images of the LAD, LCX and RCA.

3.1. *Application of contrast agent*

An extracellular contrast agent was applied in all patients and 5 healthy subjects. None of the participants experienced any adverse reaction to the contrast agent. SNR- and CNR-values were assessed before and after application of contrast agent for proximal LAD, proximal LCX and proximal RCA, separately. Table 5 summarizes the SNR- and CNR-data.

A single dose (0.1 mmol/kg) of Gd-DTPA was applied in 9 participants; a double dose of 0.2 mmol/kg was given to 10 participants. No significant differences in SNR and CNR were observed between the two groups.

In both vessels, SNR increased significantly after application of Gd-DTPA. The CNR of the RCA improved after application of this extracellular contrast agent, whereas it remained rather unchanged for LAD and LCX. The overall number of visible segments was not altered by the application of an extracellular contrast agent (71.0 ± 16.1% vs. 71.6 ± 16.3%, p = ns) nor was the image quality (Table 6, Fig. 3).

4. Discussion

In the present study, we assessed the impact of Gadolinium-DTPA on the performance of an ECG-gated, breath-hold 3D-SSFP sequence. We found that this technique allows for depiction of extensive parts of the coronary artery tree within an acceptable examination time. Despite an increase of SNR in all coronaries and an increase of CNR in the RCA, the application of an extravascular contrast agent did not significantly increase the number of visualized segments or the image quality.

Our results confirm earlier reports on a better visualization of the RCA as compared to LAD and LCX (6, 19, 20, 21), which can be explained by the location and shape of the vessels. Furthermore, our data underscore the fact that MRCA of patients is more difficult than in healthy subjects (22). In addition, we observed, that total examination times were shorter in healthy subjects (38 ± 14 min) than in patients (44 ± 9 min). This was mainly due to difficulties in holding their breath and more difficult vessel identification due to altered signal intensities.

SSFP-based sequences are known to be especially sensitive to magnetic field inhomogenities leading to off-resonance artefacts. Although careful magnetic field shimming was carried out prior to each scan in this study, a volume selective magnetic field shim of the heart was applied when severe artifacts occurred, and reduced this problem. Nevertheless, two patients had to be excluded from image analysis due to off-resonance artifacts. Another technical challenge for MRCA is coronary artery motion, which may reach a distance of up to 2 cm during the cardiac cycle. Cardiac motion is expected to be minimal in mid-diastole, although the timing of this period varies considerably between subjects (23).

We started data acquisition after a trigger delay of 60% of the RR-interval in mid-diastole. The individual optimization of the trigger delay (24) may have improved the image quality.

4.1. *Limitations*

In the present study, only feasibility has been tested; improvement of the investigational sequence has not been the aim of this work. Recently, newer technical approaches, such as the use of parallel imaging or different cardiac coils (18, 25), have been published and may be of additional value for this technique.

We did not intend to assess the diagnostic accuracy of the investigational technique and thus a careful investigation of the diagnostic performance in terms of sensitivity and specificity is required.

5. Conclusion

In conclusion, a 3D breath-hold SSFP technique may serve as a useful pulse sequence for MR Coronary Angiography. The application of an extracellular contrast agent (Gadolinium-DTPA) does not significantly improve visibility or image quality of the coronary arteries. Now that feasibility has been shown, the diagnostic performance of this technique should be tested in future studies.

6. Abbreviations

FIESTA	fast imaging employing steady-state acquisition
CNR	contrast-to-noise ratio
LAD	left anterior descending coronary artery
LCA	left coronary artery
LCX	left circumflex coronary artery
LMCA	left main coronary artery
MIP	maximum intensity projection
RCA	right coronary artery
SNR	signal-to-noise ratio
SSFP	steady state free precession

Acknowledgments

We are indebted to Kerstin Kretschel, Evelyn Polzin and Ursula Wagner for their technical assistance.

References

1. Manning WJ, Li W, Edelman RR. A preliminary report comparing magnetic resonance coronary angiography with conventional angiography. N Engl J Med 1993; 328:828–832.
2. Botnar RM, Stuber M, Danias PG, Kissinger KV, Manning WJ. Improved coronary artery definition with T2-weighted free-breathing three-dimensional coronary MRA. Circulation 1999; 99:3139–3148.
3. Boernert P, Stuber M, Botnar RM, Kissinger KV, Manning WJ. Comparison of fat suppression strategies in 3D spiral coronary magnetic resonance angiography. J Magn Reson Imaging 2002; 15:462–466.
4. Spuentrup E, Stuber M, Botnar RM, Kissinger KV, Manning WJ. Real-time motion correction in navigator-gated free-breathing double-oblique submillimeter 3D right coronary artery magnetic resonance angiography. Invest Radiol 2002; 37:632–636.
5. Stuber M, Botnar RM, Danias PG, Sodickson DK, Kissinger KV, Van Cauteren M, De Becker J, Manning WJ. Double-oblique free-breathing high resolution three-dimensional coronary magnetic resonance angiography. J Am Coll Cardiol 1999; 34:524–531.
6. Regenfus M, Ropers D, Achenbach S, Schlundt C, Kessler W, Laub G, Moshage W, Daniel WG. Comparison of contrast-enhanced breath-hold and free-breathing respiratory-gated imaging in three-dimensional magnetic resonance coronary angiography. Am J Cardiol 2002; 90:725–730.
7. Deshpande VS, Shea SM, Chung YC, McCarthy RM, Finn JP, Debiao L. Breath-hold three-dimensional true-FISP imaging of coronary arteries using asymmetric sampling. J Magn Reson Imaging 2002; 15:473–478.
8. Stuber M, Boernert P, Spuentrup E, Botnar RM, Manning WJ. Selective three-dimensional visualization of the coronary arterial lumen using arterial spin tagging. Magn Reson Med 2002; 47:322–329.
9. Wittlinger T, Voigtlander T, Rohr M, Meyer J, Thelen M, Kreitner KF, Kalden P. Magnetic resonance imaging of coronary artery occlusions in the navigator technique. Int J Cardiovasc Imaging 2002; 18:203–211.
10. Deshpande VS, Shea SM, Laub G, Simonetti OP, Finn JP, Li D. 3D magnetization-prepared trueFISP: a new technique for imaging coronary arteries. Magn Reson Med 2001; 46:494–502.
11. McCarthy RM, Shea SM, Deshpande VS, Green JD, Pereles FS, Carr JC, Finn JP, Li D. Coronary MR angiography: trueFISP imaging improved by prolonging breath holds with preoxygenation in healthy volunteers. Radiology 2003; 227:283–288.
12. Weber OM, Martin AJ, Higgins CB. Whole-heart steady-state free precession coronary artery magnetic resonance angiography. Magn Reson Med 2003; 50:1223–1228.
13. Giorgi B, Dymarkowski S, Maes F, Kouwenhoven M, Bogaert J. Improved visualization of coronary arteries using a new three-dimensional submillimeter MR coronary angiography sequence with balanced gradients. Am J Radiol 2002; 179:901–910.
14. Spuentrup E, Buecker A, Stuber M, Botnar R, Nguyen TH, Bornert P, Kolker C, Gunther RW. Navigator-gated coronary magnetic resonance angiography using steady-state free precession: comparison to standard T2-prepared gradient-echo and spiral imaging. Invest Radiol 2003; 38:263–268.
15. Barkhausen J, Ruehm SG, Goyen M, Buck T, Laub G, Debatin JF. MR evaluation of ventricular function: true fast imaging with steady-state precession versus fast low-angle shot cine MR imaging: feasibility study. Radiology 2001; 219:264–269.
16. Foo TK, Ho VB, Marcos HB, Hood MN, Choyke PL. MR angiography using steady-state free precession. Magn Reson Med 2002; 48:699–706.
17. Saranathan M, Rochitte CE, Foo TK. Fast, three-dimensional free-breathing MR imaging of myocardial infarction: a feasibility study. Magn Reson Med 2004; 51:1055–1060.
18. Niendorf T, Saranathan M, Lingamneni A, Pedrosa I, Spencer M, Cline H, Foo TK.F, Rofsky NM. Short breath-hold, volumetric coronary MR angiography employing steady-state free precession in conjunction with parallel imaging. Magn Reson Med 2005; 53:885–894.
19. Bogaert J, Kuzo R, Dymarkowski S, Beckers R, Piessens J, Rademakers FE. Coronary artery imaging with real-time navigator three-dimensional turbo-field-echo MR coronary angiography: initial experience. Radiology 2003; 226:707–716.
20. Kim WY, Danias PG, Stuber M, Flamm SD, Plein S, Nagel E, Langerak SE, Weber OM, Pedersen EM, Schmidt M, Botnar RM, Manning WJ. Coronary magnetic resonance angiography for the detection of coronary stenoses. N Engl J Med 2001; 345:1863–1869.
21. van Geuns RJ, Wielopolski PA, de Bruin HG, Rensing BJ, Hulshoff M, van Ooijen PM, de Feyter PJ, Oudkerk M. MR coronary angiography with breath-hold targeted volumes: preliminary clinical results. Radiology 2000; 217:270–277.
22. Taylor AM, Keegan J, Jhooti P, Gatehouse PD, Firmin DN, Pennell DJ. Differences between normal subjects and patients with coronary artery disease for three different MR coronary angiography respiratory suppression techniques. J Magn Reson Imaging 1999; 9:786–793.
23. Wang Y, Vidan E, Bergmann GW. Cardiac motion of coronary arteries: variability in the rest period and implications for coronary MR angiography. Radiology 1999; 213:751–758.
24. Plein S, Jones TR, Ridgway JP, Sivananthan MU. Three-dimensional coronary MR angiography performed with subject-specific cardiac acquisition windows and motion-adapted respiratory gating. Am J Radiol 2003; 180:505–515.
25. Zhu Y, Hardy CJ, Sodickson DK, Giaquinto RO, Dumoulin CL, Kenwood G, Niendorf T, Lejay H, McKenzie CA, Ohliger MA, Rofsky NM. Highly parallel volumetric imaging with a 32-element RF coil array. Magn Reson Med 2004; 52:869–877.